CONF-8806161--1

To be presented as a course at the International School of Physics Enrico Fermi, Varenna, Italy June 28 to July 7, 1988, and to appear in its Proceedings

Experimental Studies of the Chemistry of Metal Clusters[a)]

CONF-8806161--1

DE88 012034

E. K. Parks and S. J. Riley

Chemistry Division, Argonne National Laboratory, Argonne, IL 60439 USA

The procedures for studying chemical reactions of metal clusters in a continuous-flow reactor are described, and examples of such studies are given. Experiments to be discussed include kinetics and thermodynamics measurements, and determination of the composition of clusters saturated with various adsorbate reagents. Specific systems to be covered include the reaction of iron clusters with ammonia and with hydrogen, the reaction of nickel clusters with hydrogen and with ammonia, and the reaction of platinum clusters with ethylene. The last two reactions are characterized by complex, multi-step processes that lead to adsorbate decomposition and hydrogen desorption from the clusters. Methods for probing these processes will be discussed.

---

a) Work performed under the auspices of the Office of Basic Energy Sciences, Division of Chemical Sciences, U. S. Department of Energy, under Contract W-31-109-Eng-38.

I. INTRODUCTION

Recent years have seen an explosive growth in the study of isolated clusters of many chemical elements. One reason for this has been the development of the laser vaporization technique for the generation of clusters of virtually any material that can be fabricated into an appropriate target.[1] Thus even the most refractory materials can be studied. Among these are the transition metals. Since most heterogeneous catalysts consist of finely divided preparations of transition metals, such clusters appear an obvious subject for fundamental studies aimed at a deeper understanding of the molecular basis for heterogeneous catalysis. Clusters are also a natural starting point for theoretical treatments of chemical properties of metal surfaces, since the smaller clusters consist of mostly surface atoms.

Of course, chemical properties are ultimately determined by electronic properties, and there are many studies of cluster physical properties, such as measurements of ionization potentials[2] and electron affinities,[3] photophysics,[4] photoelectron spectroscopy,[5] etc. This course, however, will concentrate on the gas phase chemical reactions of transition metal clusters with simple molecules. It will begin with a characterization of the continuous-flow cluster source and reactor, including a discussion of the process of cluster

growth and reaction. After consideration of the procedure for detecting neutral clusters and their reaction products, examples of recent studies will be given. The types of experiments to be discussed include kinetics, thermodynamics, saturated product compositions, and adsorbate decomposition and desorption from cluster surfaces.

II. EXPERIMENTAL

Clusters are made and reacted in a laser-vaporization cluster source (CS) that is coupled to a flow tube reactor (FTR). Reaction products are formed into a molecular beam and transported to a laser-ionization time-of-flight (TOF) mass spectrometer for detection. Each of these components will be described in some detail below.

Figure 1 shows a schematic diagram of the combination cluster source and flow tube reactor. It is based on a 0.32 cm i.d. tube into which inert Helium carrier gas is introduced through the two ports labeled A and B and reagent gas through ports C and/or D. All gases exit through a 1 mm dia. nozzle. For the purposes of description, we term the CS the region to the left of the vertical dashed line. Essentially, the CS is the region where clusters are made, and we need to be sure that whatever processes lead to cluster formation, they have terminated before the clusters reach port C in their travel down the tube. The principal operating feature of our source that allows us to attempt to characterize it with this

much detail is that the gases are flowed continuously through it. Unlike the more usual situation of using pulsed gas valves,[6] in this case we can establish known and reproducible conditions of gas pressure and gas and cluster temperature, and can try to model the various processes occurring in the CS.

The metal to be studied is used in the form of a 0.68 cm dia. rod (or tube) located in a channel that is perpendicular to the flow tube axis and positioned so that the surface of the rod protrudes slightly into the flow tube. Metal is vaporized from this target by pulses from an excimer laser whose beam is focussed tightly onto the rod surface. The laser enters port B through a quartz window located 5.8 cm from the rod. Carrier gas is flowed down this side port to prevent vaporized metal from depositing on the window. The target rod is continuously rotated and translated to prevent the laser from burning holes in the rod's surface. Typically, an XeCl excimer laser is used, and delivers a fluence of 40 mJ/pulse onto a spot having dimensions of 0.033 cm x 0.10 cm. Weight loss experiments show that, for an iron target, each laser pulse removes about 35 ng of metal from the rod. Most evidence suggests that the principal form of this metal is neutral atoms, although small amounts of ions and larger species may be present.

Most of the targets used in this source have been made of isotopically enriched metal if the metal has several natu-

rally occurring isotopes. This is essential when dealing with multi-atom clusters, as the mass distribution of a cluster quickly becomes very broad with increasing cluster size if there are several isotopes in the target. This is illustrated in Fig. 2. The upper panel is a portion of the TOF mass spectrum recorded using a normal iron target. In addition to a large monoxide impurity, the cluster peaks are broad and show isotopic substructure. The lower panel shows the spectrum recorded using an isotopically enriched (99.87%) ^{56}Fe target. This target was fabricated from isotopically enriched iron oxide (from Oak Ridge National Laboratory) that is reduced to the pure metal and formed into a cylinder 5 cm long having a 0.04 cm wall thickness. This cylinder is then swaged onto a mandrel to form the required 0.68 cm dia. target. Other metals are treated similarly.

The metal plume that results from vaporization is initially very hot, but it is rapidly cooled by the He gas flowing down the channel. Calculations show that the heat is essentially dissipated to the channel walls within a time that corresponds to travel of a distance of 0.5 cm down the channel. Thus there is quickly established a concentration of supersaturated metal atoms, and clustering via three-body collisions begins. We estimate that under usual conditions the metal density is too low for substantial cluster-cluster collisions, so that the primary mechanism for cluster growth is addition of atoms to growing clusters. Given this scenario,

the most important operational parameter governing cluster growth is the He pressure in the channel, because this will determine the rate at which the atoms diffuse to the channel wall, where they are lost. Experiments show that the diffusion rate has an exponential dependence on the reciprocal of the He pressure. When the atom density is below a certain critical value, cluster growth can be assumed to be terminated. Of course, cluster growth itself liberates heat, but calculations show that this heat is rapidly dissipated by collisions with the He gas, so that the clusters quickly reach the temperature of the He carrier gas. Calculations also show that cluster growth will have terminated by the time the clusters reach port C if the He pressure is below 14 ± 1 Torr, and port D for pressures below 29 ± 1 Torr. These then are the conditions for operation of the CS to assure that a fully formed size distribution of ambient temperature clusters has been prepared before reagents are added to the FTR.

Reagents are then added, either as pure gases or as mixtures in He, to port C and/or D. Reagent molecules diffuse through the He, and reagent-cluster collisions occur. Most of the reactions that have been studied to date can be characterized as *chemisorptive*, i.e, reagent molecules or perhaps their decomposition products remain bound to or near the surface of the clusters, rather than permeating the cluster framework (which would essentially represent compound formation). Thus

the molecules on the clusters are often referred to as *adsorbates*. The use of two ports at different distances from the nozzle, providing different reaction times, is very important. It allows for consistency tests on reactivity measurements, permits tests for chemical equilibrium (as will be described below), and allows the study of two-reagent reactions. Port D is particularly useful for rate constant measurements in systems of high reactivity. For the usual operating conditions of the FTR, reagent addition at port C provides 1.1 msec of reagent-cluster interaction time, while port D addition gives 0.23 msec.

At the end of the FTR the clusters and their reaction products expand out of the nozzle into a vacuum chamber. This chamber must have fairly high pumping capacity to accommodate the continuous gas flows. It is separated from the next stage of differential pumping by a 2.5 mm dia. conical skimmer located 14 mm from the nozzle. After passing through additional collimators and pumping stages, the resulting molecular beam enters the ion extraction region of the TOF mass spectrometer that is located 32 cm from the nozzle. Ionization is achieved by a second excimer laser, the firing of which is delayed relative to the vaporization laser to allow the packet of clusters to travel to the spectrometer. The ions are accelerated to 3 kV and enter a 1 m long drift tube that is oriented perpendicularly to the cluster beam. Because of this orientation, deflection plates are necessary to

direct the ions to the detector, a microchannel plate, located at the end of the drift tube. Given the geometry and voltages of the TOF spectrometer, a given setting of deflection plate voltages will generally image a 20 μsec section of time-of-flight time onto the detector. This turns out to be quite convenient, because the signal acquisition electronics generally have 10 nsec resolution, translating to 2000 data points per TOF section. This number of points is compatible with the available storage in the data acquisition computer. Data is acquired and signal averaged for several thousand laser shots to yield a TOF spectrum with adequate signal-to-noise ratio. The typical repetition rate is 20 Hz, although experiments at 40 Hz can be done with the available lasers and signal acquisition electronics.

One important consideration in experiments of this type is to determine the relationship between the distribution of ion intensities in the TOF mass spectrum and the relative concentrations of the neutral species at the end of the FTR. There are essentially three places where deviations from a linear relationship can occur. In the expansion out of the nozzle, additional cluster-reagent collisions might lead to a further extent of reaction than existed within the FTR. In the flight from the nozzle to the TOF detector, some chemisorbed reagent molecules might desorb from the clusters, resulting in an apparent reduction in the extent of reaction. In the photoionization step, multiphoton processes or even the ex-

cess energy (photon energy minus cluster ionization potential) deposited in the cluster following one-photon ionization might result in loss of some adsorbate molecules. Even if this does not happen, the relationship between neutral density and ion signal involves unknown ionization efficiencies. This is of particular concern when the ionization potential, and hence presumably the ionization efficiency, is a strong function of the number of adsorbate molecules on a given cluster. For each of these possible distortions there are experimental techniques that more or less serve to test their importance. Nozzle expansion effects are probed by varying the He pressure in the FTR. Higher pressure will cool the clusters more, and if cluster-reagent collisions are occurring there is a greater likelihood for additional reaction. We find, for example, that in the reaction of ammonia with iron clusters such collisions become important for ammonia pressures above about 20 μ.[7] Because of the expansion cooling, it appears that in most cases desorption of reagent molecules in the flight to the TOF spectrometer is not significant. Again, this can be tested by varying the He pressure in the FTR. Multiphoton processes in the ionization step are tested for by increasing the ionizing laser fluence. If new species appear in the spectrum, or if existing peaks grow at different rates with fluence, then multiphoton processes are implicated. (As discussed below, they can in some cases be utilized to our advantage.) The test for one-photon desorption is to vary the photon energy (using different ex-

cimer laser wavelengths) and carefully look for changes in the observed species. This is also a test for ionization efficiency effects. If ionization probability is indeed a function of adsorbate coverage, we can usually get some measure of this by determining the total ion signal of a particular cluster as a function of coverage. With care, we can usually be fairly confident that the measured mass spectrum reflects the distribution of neutral species in the FTR.

With this understanding of the operation of the apparatus, we can now consider the sorts of experiments that can be performed. In general, experiments involve monitoring the distribution of reaction products, by following changes in relative signals in the mass spectrum, as source conditions are changed. The most common condition to be systematically varied is reagent gas partial pressure, but other conditions include interaction time, total pressure, and temperature. There are three principal types of experiment that we have defined: kinetics,[8] saturated product compositions,[9] and thermodynamics.[10] In the first, the intensity of bare cluster signal is monitored as the reagent partial pressure in the FTR is increased. By application of pseudo-first-order rate equation theory, we find that the reaction rate constant is proportional to the slope of a plot of ln(signal) vs reagent pressure. Here is where the use of continuous gas flows in the FTR is most important. We are able to determine fairly accurately the absolute reagent pressure and interaction

time, so quantitative rate constants can be calculated. Nonetheless, there are subtle effects that occur when gas flows are changed that have nothing to do with chemistry. Pressure changes in the CS can effect absolute cluster density, and turbulence at the reagent port can also change signal levels. The most accurate rate constants can be determined when there is a cluster that either does not react or is fully reacted under the conditions of the experiment. Then all other cluster signals can be referenced to this one, and most non-chemical effects will cancel out.

In saturated product composition experiments, the reagent pressure in the FTR is increased until there is no further change in the mass spectrum, indicating that the clusters are fully reacted. From the number of reagent molecules that bind to the cluster, something can be learned about cluster structure and the nature of the binding sites. Examples will be given below.

One method of measuring the thermodynamics of adsorbate binding to clusters (essentially, the binding energy) is to deliberately promote multiphoton absorption in the photoionization process. The excess energy deposited in the cluster by the extra photons is rapidly converted to heat (internal excitation). Providing the cluster-adsorbate bond is weaker than the metal-metal bonds in the cluster, this heating will result in adsorbate desorption. From the number and energy of photons absorbed and the number of adsorbates desorbed, an

estimate of the binding energy can be made. A more quantitative procedure is to model the desorption process with something like an RRKM statistical formulation.[11] In order for a desorption to be seen it has to occur within a fraction of a microsecond (the time to extract an ion in the TOF mass spectrometer). With the rate of desorption thus defined, the statistical model can, from the total excess energy in the cluster, determine the critical energy, which is the binding energy if there is no barrier to the reverse chemisorption reaction.

More recently a new experimental procedure has been developed which provides a total picture of how a cluster binds a particular adsorbate molecule.[12] The technique is to carefully follow the uptake of the adsorbate as reagent partial pressure in the FTR is increased. The pressure may have to be varied over five orders of magnitude in order to completely map out the uptake behavior. The experimentally measured parameter is the average number of adsorbate molecules for a given pressure. This number is calculated from the heights of the peaks in the mass spectrum for a given cluster, and essentially represents the extent of coverage of that cluster. These uptake plots can often provide information about the nature of the binding sites on the cluster and can indicate the existence of sites having significantly different binding behavior. Examples will be given below.

III. EXAMPLES OF MEASUREMENTS OF CLUSTER CHEMICAL PROPERTIES

The results of numerous studies of transition metal cluster reactivity can be summarized as follows: some systems are *activated*, in which reactivity is a strong function of cluster size, and others are *facile*, in which most clusters are very reactive, independent of size. There are various fates for the molecule that reacts. It may simply chemisorb nondissociatively, maintaining its chemical identity (example: ammonia on iron clusters). It may dissociatively chemisorb but have its constituents remain on the cluster (example: hydrogen on iron clusters). Or it may dissociate and lose some of its constituents (example: ammonia on nickel clusters). The latter process is quite complex, and we are still trying to understand the detailed sequence of bond breakings and formations that constitute these reactions.

Much has been said concerning activated reactions and the reason for their cluster size dependence. Initially it was noted that in some systems there can be a strong anticorrelation between reactivity and cluster ionization potential (IP).[8,13] This suggested an appealing picture, to be illustrated with the reaction of iron clusters with hydrogen. Relevant data is shown in Fig. 3. If there is a barrier to the reaction, it would presumably be the breaking of the H-H bond, since adsorption is dissociative. If an electron could be transferred from the cluster to the hydrogen molecule, this would facilitate the reaction because it would enter the

lowest unoccupied H_2 orbital, which is antibonding, thus weakening the H_2 bond. The lower the cluster IP, the easier this electron transfer, and the faster the reaction. This argument can be put on a more quantitative level by considering orbital energy levels and so on,[14] but fundamentally this is the picture. However, it is not the entire picture, since the anticorrelation is not perfect, as can be seen in Fig. 3.

We have recently done a series of studies of iron cluster reactions that suggest the underlying principal that determines reactivity and other chemical properties is geometrical structure.[15] Of course, geometrical structure and electronic properties such as IP are not uncoupled. Nonetheless we believe sudden changes in cluster properties such as reactivity, adsorbate binding energy, and IP are manifestations of structural changes. Our evidence suggests there are numerous structural changes in the growth sequence from small iron clusters to bulk metal. This emphasizes the importance of being able to prepare size-selected clusters for experimental techniques, such as optical spectroscopy, that do not incorporate built-in size selectivity, as mass spectrometry does.

One important aspect of experimental studies of cluster reactions is the determination of whether a given reaction occurs under equilibrium or kinetically limited conditions. There is a particularly simple way to do this using our continuous-flow reactor that allows reagent-cluster interaction time to be varied by adding reagent to either port C or D. If, for a

given reagent partial pressure, the composition of the products (i.e., the average number of adsorbate molecules on a given cluster) is independent of interaction time, then the system is at equilibrium. If, on the other hand, the extent of reaction changes with interaction time, with the coverage increasing with increasing time at a given pressure, then the system is kinetically limited. The iron cluster - ammonia reaction provides a particularly good example of this. One reason is that the ammonia binding energy monotonically decreases with increasing coverage. Now binding energy is directly related to whether the reaction is kinetically limited or not, because by "kinetically limited" we are really asking the question "is the lifetime for desorption longer or shorter than the time the cluster spends in the FTR?" Desorption lifetime is determined by, among other things, binding energy. The quantitative relationship can be estimated by such models as RRKM statistical treatments.[11] It turns out that typically the first 60% or so of the ammonias that bind to iron clusters have binding energies high enough that desorption lifetimes are longer than the millisecond the clusters spend in the FTR, so their addition is kinetically limited. For the remaining ammonias, the binding energies become sufficiently low that lifetimes are shorter than a millisecond, and equilibrium prevails. This distinction between kinetics and equilibrium is quite dramatic on an uptake plot, as is shown in Fig. 4. Here the average number of ammonia molecules, $\bar{m}$, is plotted vs ammonia partial pressure in

the FTR for Fe_{61}. As can be seen, in the kinetically limited region (below 2 μ), the uptake is quite rapid, and if the ammonia is added at port D it takes a larger pressure to achieve a given level of ammoniation than if it is added at port C. At higher pressures, the reaction is at equilibrium and the slope of the uptake curve is generally considerably smaller. Above 20 μ, the plot shows a plateau, representing saturation of the chemisorption sites on the cluster. At still higher pressures, the curve takes another upturn. In this case, the ammonia pressure in the FTR is high enough that substantial cooling of the clusters occurs in the nozzle expansion. This, coupled with the increased rate of ammonia - cluster collisions in the expansion, leads to the formation of a second, physisorbed layer of molecules on the cluster surface.

Composition data in the equilibrium region can be used to determine equilibrium thermodynamic properties such as the standard free energy of chemisorption. This will be illustrated for the iron cluster-ammonia system. If the assumption is made that at a value of $\bar{m}$ = m-1/2 the $Fe_n(NH_3)_{m-1}$ and $Fe_n(NH_3)_m$ species have equal concentrations in the flow tube, then the standard free energy for the addition of the m'th ammonia is just given by[16]

$$\Delta G^\circ = RT \ln P(NH_3)$$

where $P(NH_3)$ is the ammonia partial pressure giving the corresponding $\bar{m}$ value. Of course, what is really desired is the *enthalpy* of chemisorption. To get this, the entropy of chemisorption must be determined. One way is to study the temperature dependence of the reaction. Another is to estimate the entropy from the various degrees of freedom in the system. When this is done,[16] we find that the range of binding energies of ammonia to iron clusters is quite small, varying by no more than 15% between Fe_{10} and Fe_{85}. The data does show local maxima that can be correlated with clusters of particular stability as determined by other methods. The relative insensitivity of binding energy to cluster size (and the fact that the binding energies are similar to those found for bulk iron[17]) suggests that the ammonia-iron interaction is similar in all cases and may be fairly localized. The observation that ammonia chemisorption lowers iron cluster ionization potentials (as well as the bulk iron work function[18]) suggests that the bonding occurs via donation of lone pair electrons on the nitrogen to unfilled d shells of the surface iron atoms. This similarity of bonding may also explain why the ammonia - iron cluster reaction is facile, i.e., shows little cluster-size dependence, in the kinetically limited region.

As an example of saturated cluster composition, consider the reaction of iron and nickel clusters with hydrogen.[19] Since these are assumed to be surface reactions, it is convenient

to compare the number of adsorbates at saturation with some measure of the number of surface metal atoms on the clusters. The structureless packing model[9] provides such a measure. As shown in Fig. 5, an interesting difference is found between nickel and iron. Nickel clusters are essentially "covered" with hydrogens at saturation; there are as many hydrogen atoms as surface nickel atoms. Iron clusters, on the other hand, are less than fully covered, and in fact show proportionately less fractional coverage with increasing size, being 1.0 at Fe_{40} and 0.8 at Fe_{250}. This difference is reminiscent of another difference between nickel and iron seen in the heterogeneously catalyzed reduction of CO by hydrogen (the Fischer-Tropsch synthesis). Nickel catalysts usually lead to the production of methane, while iron catalysts often result in higher hydrocarbons, even waxes.[20] In the context of the cluster studies, we would postulate that on the fully hydrogenated nickel catalyst the CO molecules will be surrounded by hydrogens, and only C-H bond formation is possible. On the less than fully covered iron catalyst, however, there is a chance for CO molecules to occupy adjacent sites, allowing the formation of C-C bonds and the production of higher hydrocarbons.

Saturation studies of ammonia on iron clusters likewise show a decreasing fractional coverage with increasing cluster size, going from greater than one ammonia per three surface iron atoms for clusters smaller than Fe_{100} to less than 1/3

for larger clusters.[7] Eventually, on bulk iron, the ratio is known to be 1/6.[17] This is presumably an indication of the curvature of the cluster surface. Smaller clusters have greater curvature, and fractionally more ammonias can be accommodated before mutual repulsion limits their binding. Repulsive forces between adsorbate molecules are also consistent with a monotonic decrease in binding energy with increasing coverage, a conclusion of the uptake experiments described above.

Another experiment has been done in which iron clusters saturated with ammonia are exposed to high pressures of deuterium. While in general it takes somewhat higher deuterium pressures to saturate the ammoniated clusters than the bare clusters, the saturated compositions are essentially the same as for clusters without ammonia, as is shown in Fig. 6. In addition, the clusters adsorb the deuteriums with the loss of at most one or two ammonias. In fact, the final composition of the doubly saturated clusters is essentially independent of the order in which the reagents are added. These results indicate that deuterium (and hence, hydrogen) and ammonia bind to iron clusters noncompetitively, i.e., to different sites. This is consistent with the generally accepted picture of hydrogen binding to multi-atom sites[21] while ammonia prefers atop or single-atom sites.[22] Thus we see that uptake experiments can tell us something about the nature of cluster binding sites and, perhaps in some cases, cluster structure.

Another important class of cluster chemical reactions is one in which chemisorption is followed by (or is perhaps coincident with) adsorbate decomposition. Subsequently (or again perhaps concertedly) products of the decomposition desorb from the cluster. Most examples of such processes involve hydrogen-containing adsorbates and loss of hydrogen molecules, and include benzene on niobium clusters[23] and ammonia and ethylene on nickel and platinum clusters. In the case of ethylene reacting with platinum clusters, we find that when ethylene is added to port C or D, product compositions (i.e., the number of C_2 units) are invariant to a 50-fold increase in ethylene pressure, indicating saturation and hence presumably equilibrium. However, as is shown in Fig. 7, the products contain fewer C_2 units if the reagent is added at port D, indicating a kinetic limitation. How can both apparent equilibrium and kinetics coexist? It suggests the overall decomposition/desorption process contains several steps, at least one of which is rate limiting, or slow on the msec timescale. Although the data is not quite definitive (isotopically enriched platinum was not used, so the mass peaks are quite broad), it appears the number of hydrogens lost from a cluster having a given number of C_2 units is independent of the interaction time. This means that the hydrogen desorption step is not the rate limiting one. Since other studies (such as H/D exchange on iron clusters[24]) have shown that hydrogen migration on cluster surfaces can be rapid, this suggests that the rate limiting step is either

the C-H bond breakage or the H-H bond formation. In addition, the fact that the number of C_2 units found on a cluster depends on time but not pressure implies the product of the decomposition must bind to a different site than the initial ethylene, and that the initial ethylene binding is rapid at the ethylene pressures studied. The longer the time, the more ethylenes that can decompose, and the more additional ethylenes that can bind. But for a given time, only so many ethylenes can decompose and only so many additional ethylenes can bind. An additional tantalizing aspect of this reaction is that even when only one ethylene is bound to a cluster, it appears that it loses an H_2 molecule. This would seem to rule out the presence of the famous ethylidyne (C_2H_3) intermediate[25] under the conditions of these experiments.

The case of ammonia reacting with nickel clusters provides us with more detailed information, since we have isotopically pure targets and superior mass resolution. We find that the maximum number of hydrogens lost from a given cluster depends linearly on the number of "ammonias" on the cluster. As shown in the upper panel of Fig. 8, when the ammonia is added to port C, $Ni_7(NH_3)_7$ shows peaks in the mass spectrum corresponding to loss of 0, 1, 2, and 3 hydrogen molecules; $Ni_7(NH_3)_6$ has 0, 1, and 2; $Ni_7(NH_3)_5$ has 0 and 1; and $Ni_7(NH_3)_4$ loses no hydrogens. One possible interpretation of this is that the decomposition terminates at NH, and that the maximum number of hydrogens that can result from decomposition *and*

remain bound to the Ni_7 cluster is eight. Thus, for example, the $Ni_7(NH_3)_6$ species that has lost two H_2 molecules is best thought of as $Ni_7(NH)_6H_8$. Eight is the approximate number of H atoms found on a Ni_7 cluster that is saturated with hydrogen.[26] These observations suggest that hydrogens and NH radicals bind to different sites. As for ethylene - platinum, the pattern of peaks seen in the mass spectrum with port C addition is essentially unchanged when the ammonia pressure is increased 9-fold, indicative of saturation. When, however, the ammonia is added to port D, most indications of hydrogen loss disappear (the lower panel in Fig. 8). The kinetic effect is clearly more dramatic in this case than for ethylene - platinum. Also, there does not appear to be a difference in the average number of ammonias (or nitrogens) bound to the clusters whether or not there is extensive decomposition/desorption. Thus we conclude that in this case the nitrogen-containing species bind to the same sites before and after decomposition.

These adsorbate decomposition studies represent just the beginning of what will probably be an extensive series of experiments aimed at determining the detailed sequence of steps that constitute the overall decomposition and desorption process. These reactions are prototypical examples of the sorts of chemical bond breaking and making that can be catalyzed by metal surfaces. The challenge in the years to come is to develop a set of experimental tools that will enable us to un-

derstand these reactions at the level that we presently understand the non-dissociative chemisorption reactions. It promises to be an exciting period.

IV. CONCLUSION

The new field of metal cluster chemistry has already proven to be fruitful, challenging, and exciting. In many respects clusters represent a new class of chemical reagents whose properties we are just beginning to understand. While transition metal clusters serve as obvious models for heterogeneous catalysis, a better understanding of their chemical and physical properties will also impact the areas of surface science, solid-state physics, corrosion, aerosol formation, and microelectronics. While working towards finding practical applications of metal clusters, we have discovered that they provide fascinating insights into fundamental chemical reactivity. The field will undoubtedly continue to grow and to provide us with valuable new scientific findings.

ACKNOWLEDGMENTS

We thank Dr. W. F. Hoffman III for the collection and analysis of the $Ni_n + NH_3$ data.

---

[1] T. G. Dietz, M. A. Duncan, D. E. Powers, and R. E. Smalley: *J. Chem. Phys.* 74, 6511 (1981).

[2] a) E. A. Rohlfing, D. M. Cox, and A. Kaldor: *Chem. Phys. Lett.* 99, 161 (1983); b) E. A. Rohlfing, D. M. Cox, A. Kaldor, and K. H. Johnson: *J. Chem. Phys.* 81, 3846 (1984); c) E. A. Rohlfing, D. M. Cox, and A. Kaldor: *J. Phys. Chem.* 88, 4497 (1984); d) R. L. Whetten, M. R. Zakin, D. M. Cox, D. J. Trevor, and A. Kaldor: *J. Chem. Phys.* 85, 1697 (1986).

[3] L.-S. Zheng, C. M. Karner, P. J. Brucat, S. H. Yang, C. L. Pettiette, and R. E. Smalley: *J. Chem. Phys.* 85, 1681 (1986).

[4] P. J. Brucat, L.-S. Zheng, C. L. Pettiette, S. Yang, and R. E. Smalley: *J. Chem. Phys.* 84, 3078 (1986).

[5] S. H. Yang, C. L. Pettiette, J. Conceicao, O. Chesnovsky, and R. E. Smalley: *Chem. Phys. Lett.* 139, 233 (1987).

[6] M. E. Geusic, M. D. Morse, S. C. O'Brien, and R. E. Smalley: *Rev. Sci. Instrum.* 56, 2124 (1985).

[7] E. K. Parks, G. C. Nieman, L. G. Pobo, and S. J. Riley: *J. Chem. Phys.* 88, 0000 (1988).

[8] S. C. Richtsmeier, E. K. Parks, K. Liu, L. G. Pobo, and S. J. Riley: *J. Chem. Phys.* 82, 3659 (1985).

[9] E. K. Parks, K. Liu, S. C. Richtsmeier, L. G. Pobo, and S. J. Riley: *J. Chem. Phys.* 82, 5470 (1985).

[10] K. Liu, E. K. Parks, S. C. Richtsmeier, L. G. Pobo, and S. J. Riley: *J. Chem. Phys.* 83, 2882 (1985).

[11] R. D. Levine and R. B. Bernstein: *Molecular Reaction Dynamics* (Oxford, 1974), p. 223; W. L. Hase: in *Dynamics of*

Molecular Collisions, Part B, edited by W. H. Miller (New York, 1976), p. 121.

[12] E. K. Parks, G. C. Nieman, L. G. Pobo, and S. J. Riley: *J. Chem. Phys.* 86, 1066 (1987).

[13] R. L. Whetten, D. M. Cox, D. J. Trevor, and A. Kaldor: *Phys. Rev. Lett.* 54, 1494, (1985).

[14] D. J. Trevor and A. Kaldor: *ACS Symp. Ser.* 333, 43, (1987).

[15] E. K. Parks, B. H. Weiller, P. S. Bechthold, W. F. Hoffman, G. C. Nieman, L. G. Pobo, and S. J. Riley: *J. Chem. Phys.* 88, 1622 (1988).

[16] E. K. Parks, R. Miranda, G. C. Nieman, and S. J. Riley: to be published.

[17] M. Grunze, F. Bozso, G. Ertl, and M. Weiss: *Appl. Surf. Sci.* 1, 241 (1978).

[18] M. Weiss, G. Ertl, and F. Nitschike: *Appl. Surf. Sci.* 2, 614 (1978).

[19] E. K. Parks, G. C. Nieman, L. G. Pobo, and S. J. Riley: *J. Phys. Chem.* 91, 2671 (1987).

[20] H. H. Storch, N. Golumbic, and R. B. Anderson: *The Fischer-Tropsch and Related Syntheses*, (New York, 1951), p. 7.

[21] S. P. Walch: *Surf. Sci.* 143, 188 (1984).

22 W. Erley and H. Ibach: *J. Electron. Spec. Rel. Phenom.* 31, 161 (1983).

23 R. J. St. Pierre and M. A. El-Sayed: *J. Phys. Chem.* 91, 763 (1987); R. J. St. Pierre, E. L. Chronister, and M. A. El-Sayed: *J. Phys. Chem.* 91, 5228 (1987); M. R. Zakin, D. M. Cox, and A. Kaldor: *J. Phys. Chem.* 91, 5224 (1987).

24 S. J. Riley and E. K. Parks: in *Physics and Chemistry of Small Clusters*, edited by P. Jena, B. K. Rao, and S. N. Khanna (New York, 1987), p. 727.

25 G. A. Somorjai, M. A. Van Hove, and B. E. Bent: *J. Am. Chem. Soc.* 92, 973 (1988).

26 Unpublished results.

Figure Captions

Fig. 1. Schematic diagram of the cluster source - flow-tube reactor.

Fig. 2. Portions of time-of-flight mass spectra illustrating the effect of using isotopically enriched metal targets. The upper spectrum was recorded with a normal iron target rod in the cluster source. The secondary peaks in each case are cluster monoxides. The lower spectrum is the result of using an enriched ^{56}Fe target. In this case the level of oxide impurities is significantly lower than in the top spectrum.

Fig. 3. A comparison of the reactivity of iron clusters towards hydrogen (left scale) and the cluster ionization potentials (right scale), as a function of cluster size. Reactivity is measured by the absolute pseudo-first-order rate constant for the addition of the first hydrogen molecule to the bare cluster. Data is from Ref. 24. The ionization potential data is from Ref. 2b.

Fig. 4. The uptake plot for Fe_{61} reacting with ammonia. The vertical scale gives the average number of ammonia molecules bound to the cluster for the ammonia partial pressure in the FTR shown on the horizontal scale. Below a pressure of 2 μ, the extent of uptake is different for reagent addition at ports C and D, indicating the reaction is kinetically limited

for the D port. Kinetic limitation for the C port, indicated by a change in slope, comes at about 0.3 μ. Above 20 μ, the data shows a plateau, indicating saturatior. Above about 700 μ, the data again shows increasing uptake. This is caused by substantial cooling in the nozzle expansion at these high ammonia pressures, leading to the beginning of the formation of a second, physisorbed layer of ammonia on the cluster. (Adapted from Ref. 7.)

Fig. 5. A comparison of the composition of iron and nickel clusters saturated with hydrogen and/or deuterium. Iron cluster hydride compositions are shown for clusters smaller than Fe_{132}, deuteride compositions for larger clusters. For nickel, photoionization of the saturated deuterated clusters could not be achieved for clusters smaller than Ni_{40} for the ionization laser used in these studies. (Adapted from Ref. 19.)

Fig. 6. The filled circles show the average numbers of D atoms on iron clusters saturated with deuterium. The open circles show the corresponding numbers on clusters already saturated with ammonia.

Fig. 7. A comparison of the TOF spectra observed when ethylene is reacted with platinum clusters via port C addition (upper spectrum) and port D addition (lower spectrum). Note that the ethylene pressure in the lower case is ten times that in the upper, corresponding to substantially higher

exposure (pressure times interaction time) for the port D addition. The number of C_2 units on major peaks is shown for each cluster.

Fig. 8. Spectra showing decomposition and H_2 desorption when ammonia is reacted with nickel clusters via port C addition (upper spectrum), and the absence of desorption for port D addition (lower spectrum). In the upper spectrum, the number of H atoms desorbed (as H_2 molecules) is indicated for the Ni7(NH3)7 species. (The peak to the left of the -6 peak is not -8, but is in fact $Ni_8(NH_3)_3$, as determined from isotope substitution studies.) The pattern of peaks is the same for the other species, with the 0 hydrogen loss peak being the furthest to the right in each case. For the pressures used, the ammonia exposure is approximately the same for both spectra.

CLUSTER SOURCE - FLOW-TUBE REACTOR

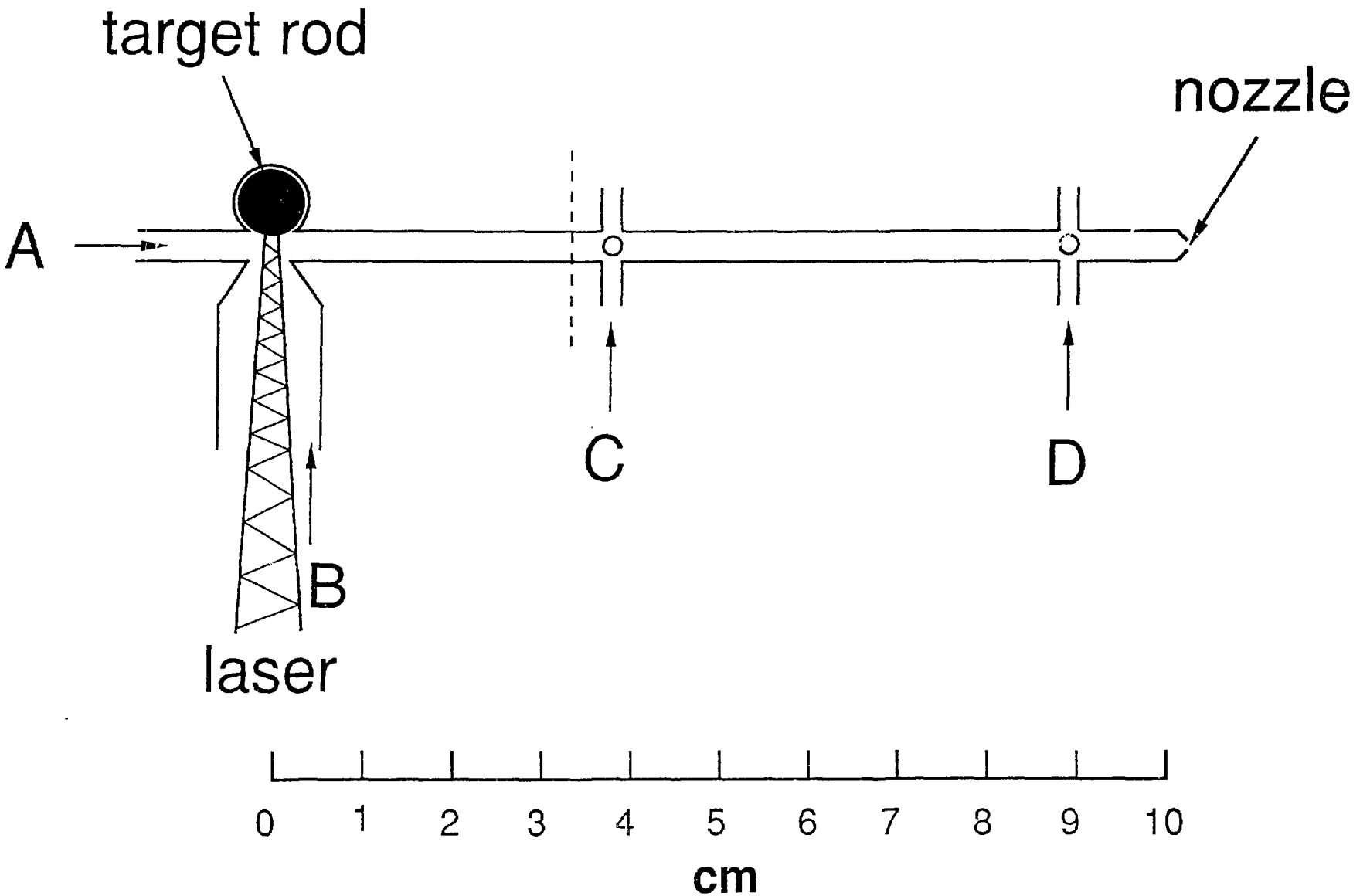

Fig. 1

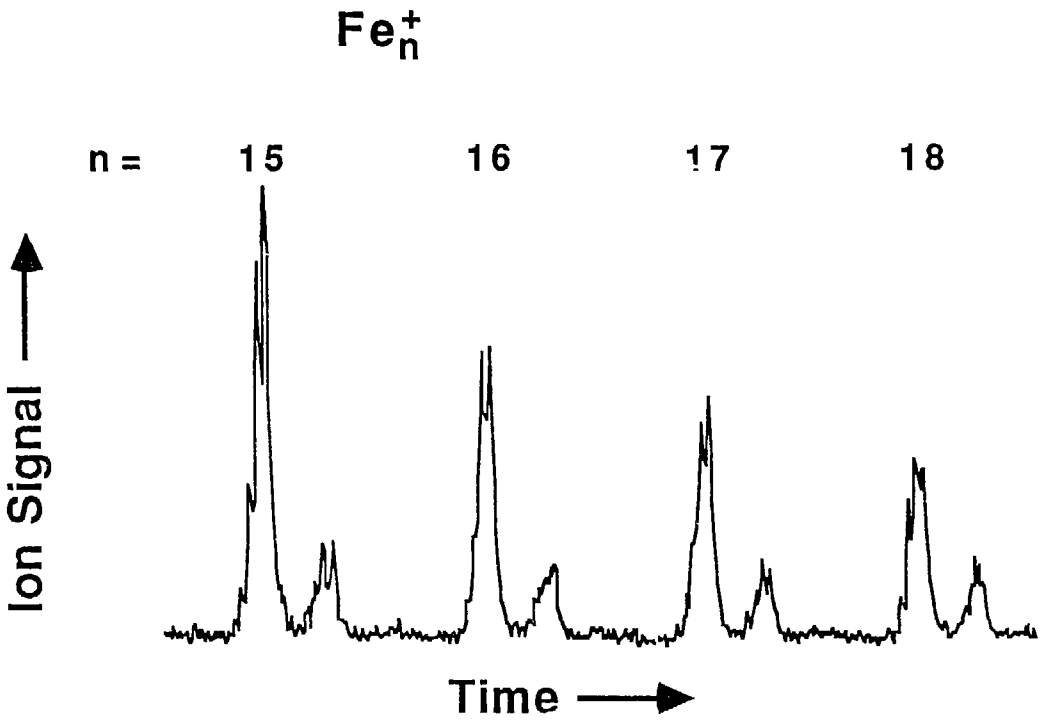

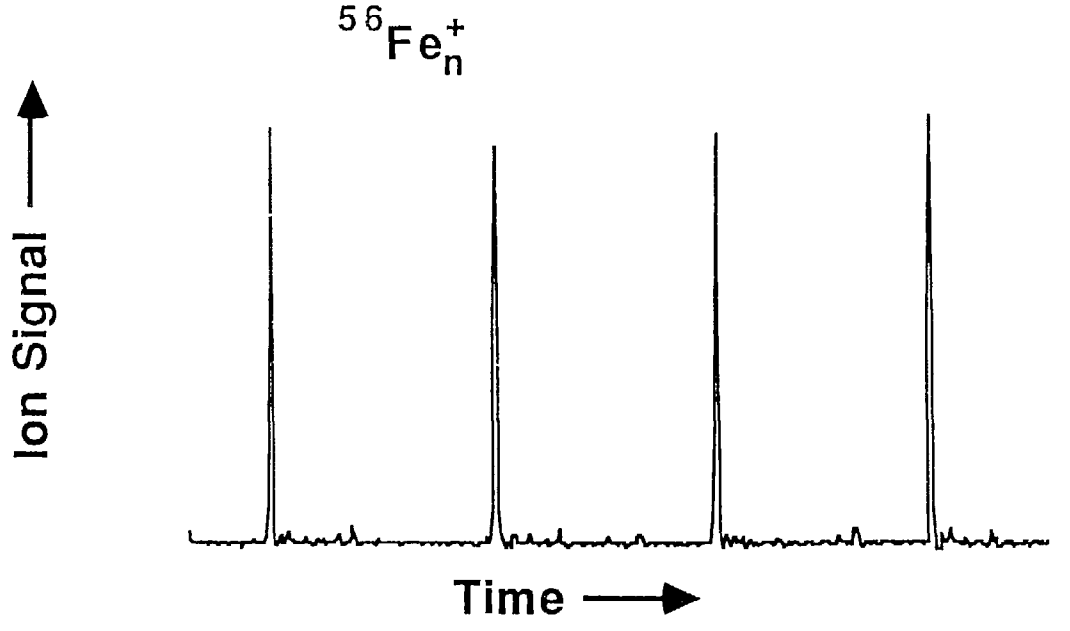

Fig. 2

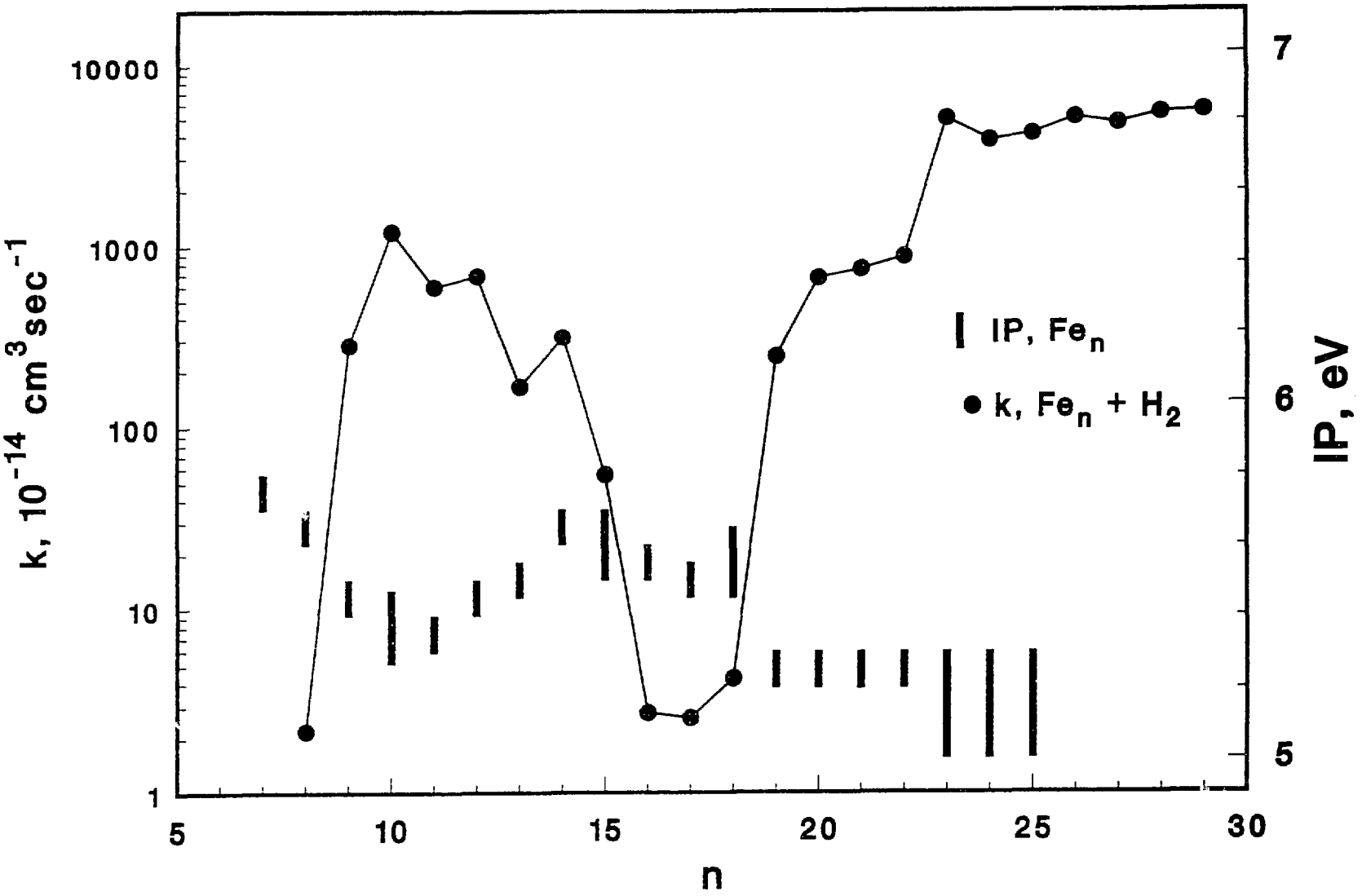
10000
1000
100
10
1
k, 10^{-14} $cm^3 sec^{-1}$
5
10
15
20
25
30
n
7
6
5
IP, eV
IP, Fe_n
k, $Fe_n + H_2$

Fig. 3

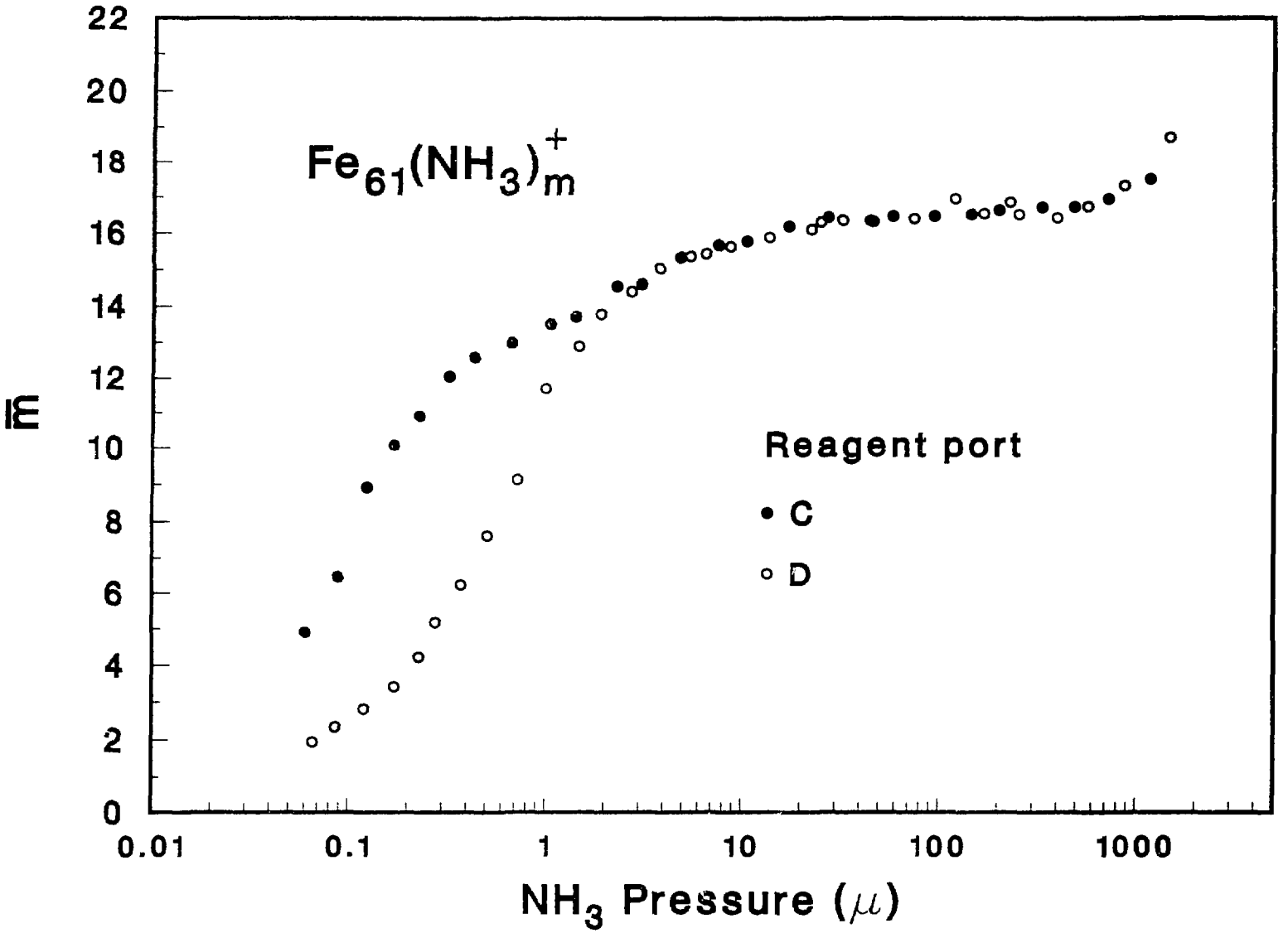
$Fe_{61}(NH_3)_m^+$
m
Reagent port
C
D
0
2
4
6
8
10
12
14
16
18
20
22
0.01
0.1
1
10
100
1000
NH_3 Pressure (μ)

Fig. 4

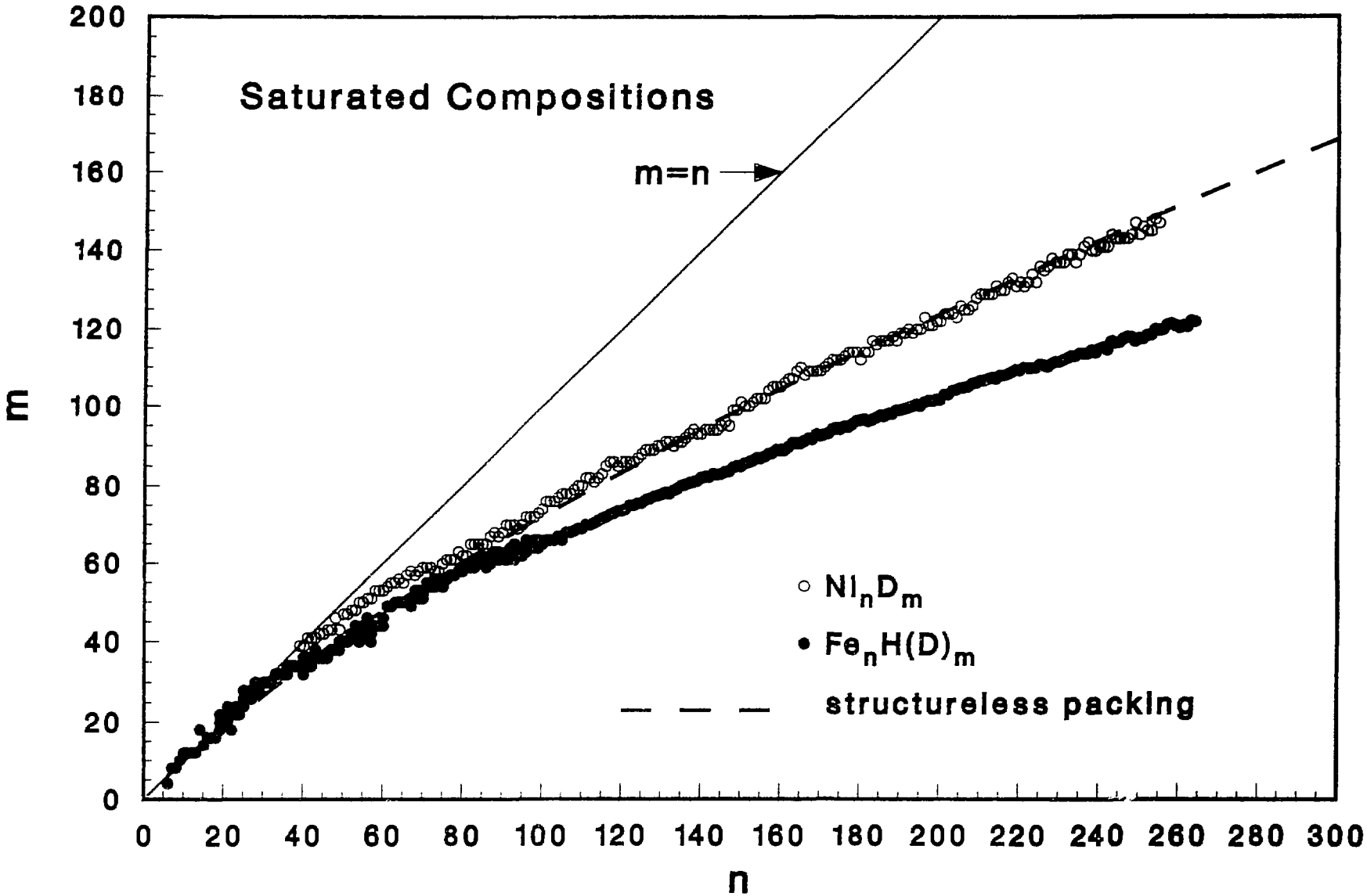
Saturated Compositions
m=n
m
n
0
20
40
60
80
100
120
140
160
180
200
220
240
260
280
300
NI_nD_m
$Fe_nH(D)_m$
structureless packing

Fig. 5

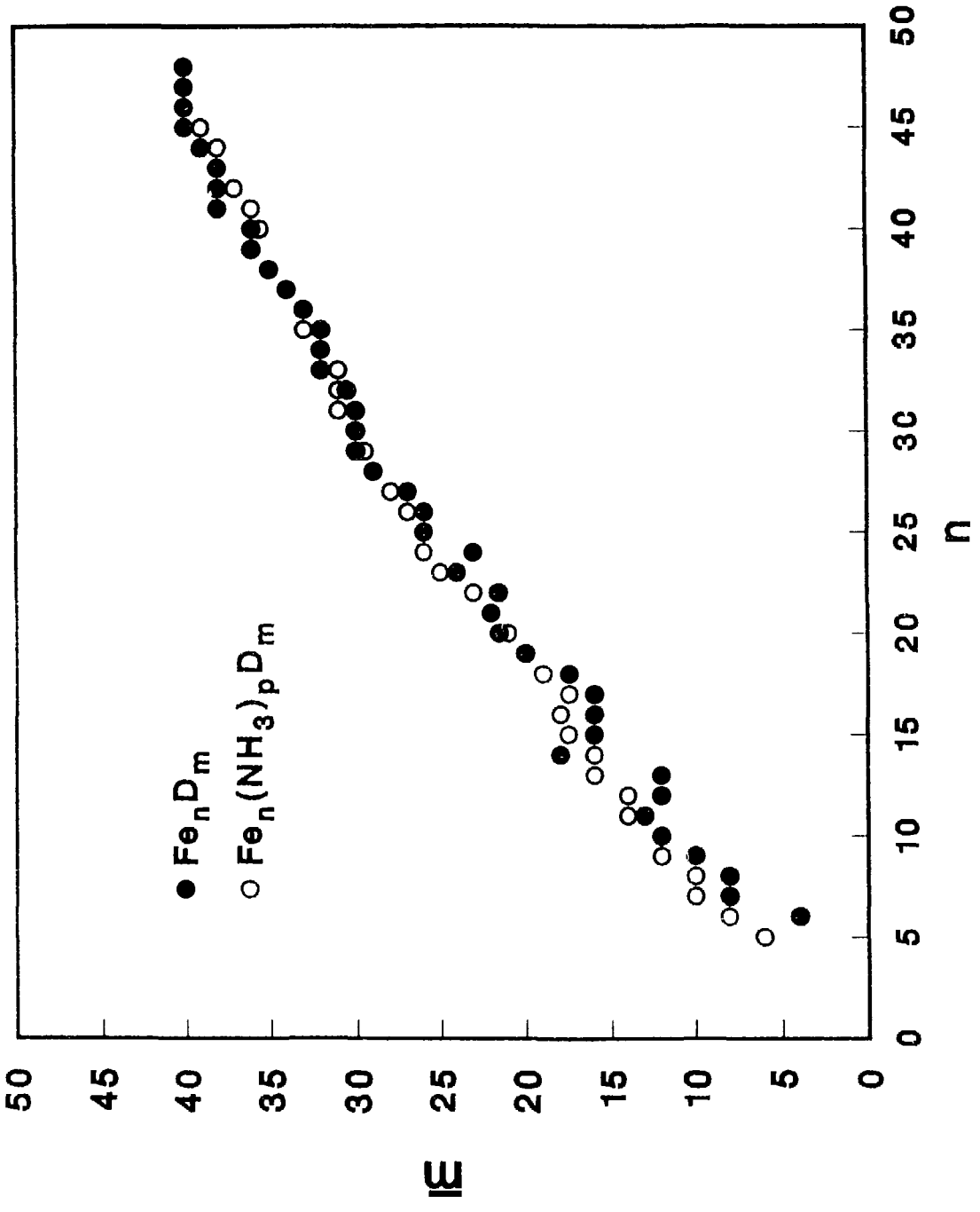

Fig. 6

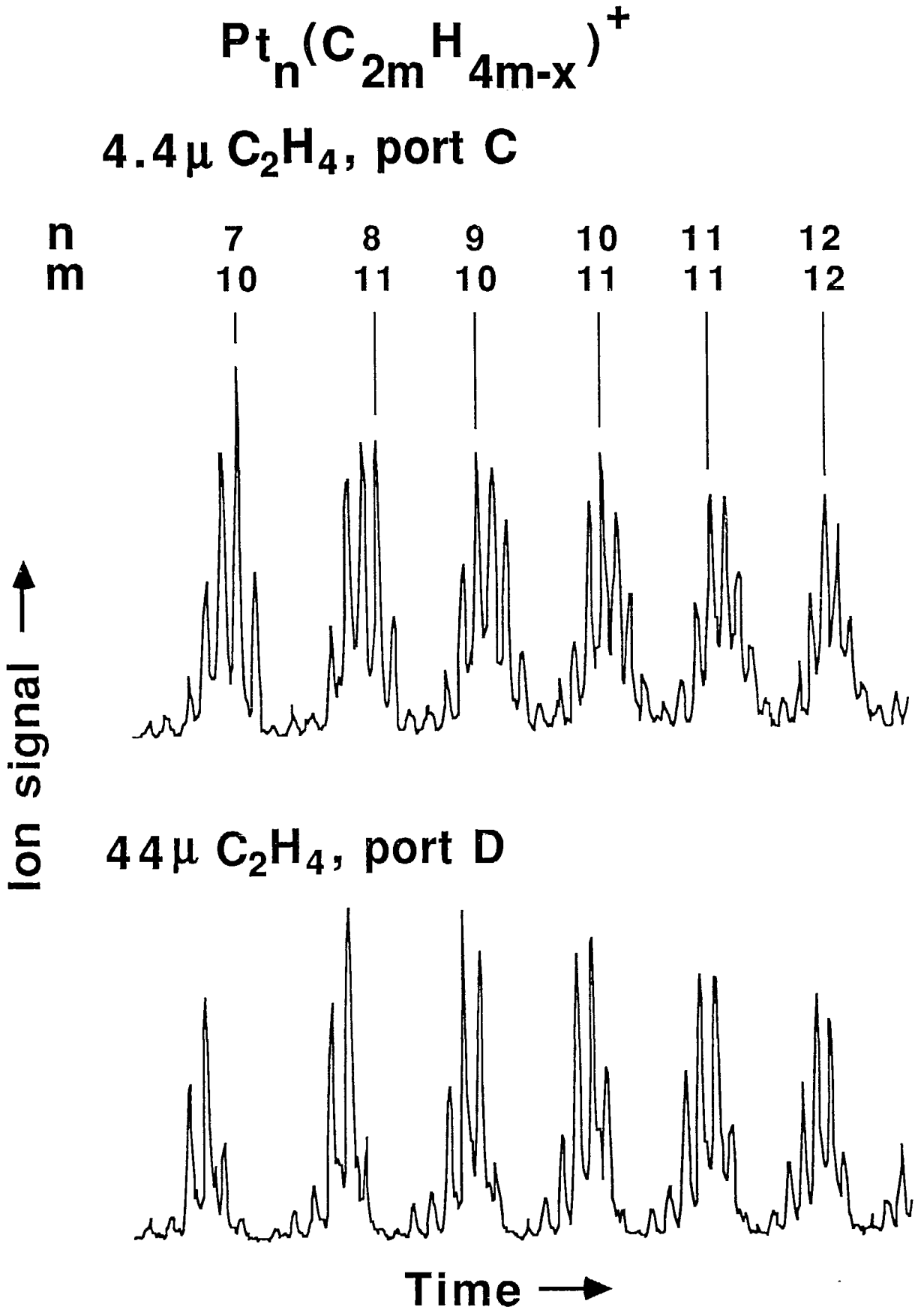
$Pt_n(C_{2m}H_{4m-x})^+$
4.4μ C_2H_4, port C
n 7 8 9 10 11 12
m 10 11 10 11 11 12
Ion signal
44μ C_2H_4, port D
Time

Fig. 7

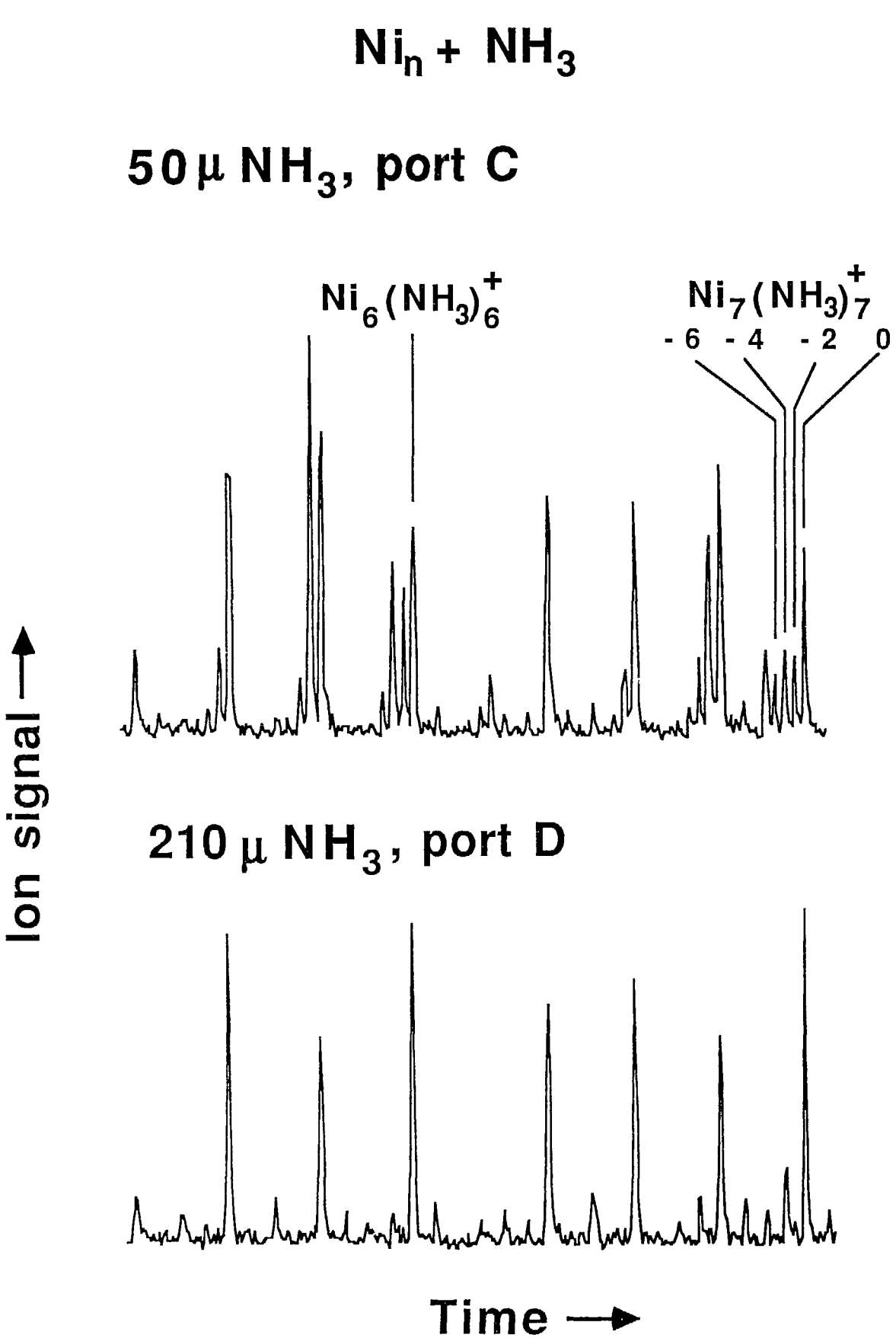
$Ni_n + NH_3$
50 μ NH_3, port C
$Ni_6(NH_3)_6^+$
$Ni_7(NH_3)_7^+$
- 6
- 4
- 2
0
Ion signal
210 μ NH_3, port D
Time

Fig. 8